considered separately correctly predict the position of substitution. In fact, no reactivity index reliable for both molecules was found in the population analyses of the reactant wave functions.

Electron distribution in the highest occupied, or frontier, orbital has been proposed[10] to be a significant factor in the outcome of electrophilic substitution reactions. The highest occupied orbitals in fluoro- and chlorobenzene are the b_2 and a_2 orbitals derived from the degenerate 3_{1g} orbitals of benzene. The b_2 orbital atomic populations (not shown) predict the order of substitution correctly, with the exception that the ipso population appears second to para; furthermore, there is a near degeneracy with the a_2 orbital which has a node at the ipso and para carbons. When the populations in the a_2 and b_2 orbitals are added, the predicted order of substitution is also incorrect.

Core orbital energies of the ring carbon atoms of aromatic reactants are commonly employed to predict the preferred position for electrophilic substitution.[22,31] The use of these energies to predict reactivity is based on the dual assumptions that a more negative carbon atom has a higher core orbital energy and that electrophilic substitution takes place at the most negative position, that is, at the carbon with the highest energy core orbital. The association holds for fluorobenzene (Table IIS and ref 22), but not for chlorobenzene.

It was shown in the section on energies that there is a correlation between the stability of a benzenium ion and substitutional preference. It is not surprising, then, that there are trends in the electron populations of the ions that correlate with the rates of reaction. The gross atomic charges of the benzenium ions (Table IV) show that the positive charge of the proton is distributed among the peripheral atoms, the hydrogens and the halogen. There are only small differences between the ions in their hydrogen charges, but there is a systematic variation in their halogen charges. The halogen atom with the least negative charge is in the *p*-halobenzenium ion followed by that in the *o*-halobenzenium ion. The halogen in *m*-halobenzenium ion is considerably more negative than the others. The π overlap populations and gross σ charges are in the same order. The π overlap population is negative in *m*-halobenzenium ion.

The ability of the halogen to participate in the π system of the ring determines the stability of a particular benzenium ion, which in turn relates to the tendency of a substituted benzene to undergo protonation at the corresponding site. The traditional quinoid structures for the σ complex,[4] derived from resonance theory, are consistent with this interpretation, except that they do not distinguish between ortho and para species.

Acknowledgments. We are grateful to Dr. N. E. Ertz for many helpful discussions and assistance with the computer coding. This work was supported in part by a grant from the National Science Foundation. Computer time was provided by the Graduate College of the University of Iowa.

Supplementary Material Available: Tables of orbital energies for all species studied (Tables IS–VS) (4 pages). Ordering information is given on any current masthead page.

References and Notes

(1) M. J. S. Dewar, *J. Chem. Soc.*, 406, 777 (1946).
(2) G. A. Olah, *J. Am. Chem. Soc.*, **94**, 808 (1972).
(3) L. M. Stock, *Prog. Phys. Org. Chem.*, **12**, 21 (1976).
(4) G. W. Wheland, *J. Am. Chem. Soc.*, **64**, 900 (1942).
(5) W. J. Hehre and J. A. Pople, *J. Am. Chem. Soc.*, **94**, 6901 (1972).
(6) W. C. Ermler, R. S. Mulliken, and E. Clementi, *J. Am. Chem. Soc.*, **98**, 388 (1976).
(7) G. A. Olah, R. H. Schlosberg, R. D. Porter, Y. K. Mo, D. P. Kelley, and G. D. Mateescu, *J. Am. Chem. Soc.*, **94**, 2034 (1972).
(8) G. A. Olah and T. E. Kiovsky, *J. Am. Chem. Soc.*, **89**, 5692 (1967).
(9) N. C. Baenziger and A. D. Nelson, *J. Am. Chem. Soc.*, **90**, 6602 (1968).
(10) K. Fukui, T. Yonezawa, and H. Shingu, *J. Chem. Phys.*, **20**, 722 (1952).
(11) A. Streitwieser, "Molecular Orbital Theory for Organic Chemists", Wiley, New York, 1961.
(12) W. C. Ermler and R. S. Mulliken, *J. Am. Chem. Soc.*, **100**, 1647 (1978).
(13) W. J. Hehre, R. T. Mciver, Jr., J. A. Pople, and P. v. R. Schleyer, *J. Am. Chem. Soc.*, **96**, 7162 (1974).
(14) S. Huzinaga, *J. Chem. Phys.*, **42**, 1293 (1965).
(15) T. H. Dunning, *J. Chem. Phys.*, **53**, 2823 (1970).
(16) A. Veillard, *Theor. Chim, Acta*, **12**, 405 (1968).
(17) T. H. Dunning, *Chem. Phys. Lett.*, **7**, 423 (1970).
(18) D. B. Neumann, H. Basch, R. L. Kornegay, L. C. Snyder, J. W. Moskowitz, C. Hornback, and S. P. Liebmann, Program 199, Quantum Chemistry Program Exchange, Indiana University, Bloomington, Ind.
(19) L. E. Sutton, "Tables of Interatomic Distances", *Chem. Soc., Spec. Publ.* **No. 18** (1965).
(20) L. Nygaard, I. Bojesen, T. Pedersen, and J. Rastrup-Andersen, *J. Mol. Struct.*, **2**, 209 (1968).
(21) I. Fischer-Hjalmars and P. Siegbahn, *Theor. Chim. Acta*, **31**, 1 (1973).
(22) D. T. Clark, D. Kilcast, D. B. Adams, and I. Scanlan, *J. Electron Spectrosc. Relat. Phenom.*, **1**, 153 (1972/3).
(23) Y. K. Lau and P. Kebarle, *J. Am. Chem. Soc.*, **98**, 1320 (1976).
(24) R. Yamdagni and P. Kebarle, *J. Am. Chem. Soc.*, **98**, 7452 (1976).
(25) A. D. Baker, D. P. May, and D. W. Turner, *J. Chem. Soc. B*, 22 (1968).
(26) R. S. Mulliken, *J. Chem. Phys.*, **23**, 1833 (1955).
(27) T. Fujita and T. Nishioka, *Prog. Phys. Org. Chem.*, **12**, 49 (1976).
(28) H. Spiesecke and W. G. Schneider, *J. Chem. Phys.*, **35**, 731 (1961).
(29) G. L. Nelson and E. A. Williams, *Prog. Phys. Org. Chem.*, **12**, 229 (1976).
(30) R. O. C. Norman and R. Taylor, "Electrophilic Substitution in Benzenoid Compounds", American Elsevier, New York, 1965.
(31) R. J. Buenker and S. D. Peyerimhoff, *Chem. Phys. Lett.*, **3**, 37 (1969).

Metallacyclopentanes and Bisolefin Complexes

Armel Stockis and Roald Hoffmann*

Contribution from the Department of Chemistry, Cornell University, Ithaca, New York 14853. *Received October 9, 1979*

Abstract: The reaction path for the bisethylene metallacyclopentane interconversion is explored, for the specific case of two olefins coordinated to a trigonal bipyramidal iron tricarbonyl. If the ethylene is unsymmetrically substituted, the reaction should proceed stereoselectively, placing the substituents so that the ethylene π^* enters the reaction with its largest lobe β to the metal in the product metallacycle. A special case of this regularity is that heteroatoms more electronegative than carbon should preferentially go in α sites, donor substitutents on α carbons, acceptor substituents on β sites.

Metallacyclopentanes have been proposed or demonstrated to be key intermediates in numerous metal-catalyzed cycloadditions and cycloreversions of olefins. Stone,[1] Wilkinson,[2] and co-workers had already prepared the first such compounds, **1** and **2**, from perfluoroethylenes by 1961, and subsequently synthesized many others.[3] Substantial interest

0002-7863/80/1502-2952$01.00/0

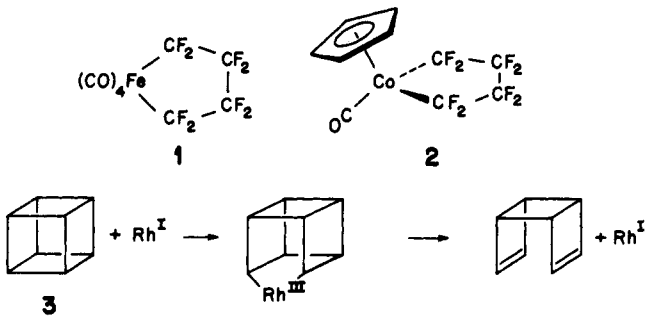

in this area of organometallic chemistry was aroused 8 years later when Halpern and Eaton reported on the rhodium(I)-catalyzed ring opening of cubane (**3**).[4]

From titanium[5] and tantalum[6] to iridium,[7] platinum,[8] nickel,[9] and copper,[10] five-membered metallacycles are isolable or probable intermediates in numerous transition-metal reactions.[11] The routes in and out of the metallacyclopentane–bisolefin system are outlined in Scheme I. Clearly this useful transformation is a link between diverse classes of organic compounds.

One well-documented case with synthetic implications is the formation of cyclopentanones from olefins, by a sequence involving coupling of two olefins into a metallacycle, CO insertion, and reductive elimination of the metal. Laszlo and Weissberger,[12] Schmid,[13] Grevels and Koerner von Gustorf,[14] and their co-workers have devised such reactions using inexpensive $Fe(CO)_5$.[15] Although there might be dozens of isomeric products when asymmetric olefins are employed (up to a score known[12c,f]) the reactions are usually stereospecific, by a happy combination of electronic and steric effects. A summary of what has been learned about one system is given in Scheme II. Most intermediates of this reaction have been characterized at low temperatures,[14] and the structure of one compound, boxed, has been determined by X-ray crystallography.[16]

Scheme I

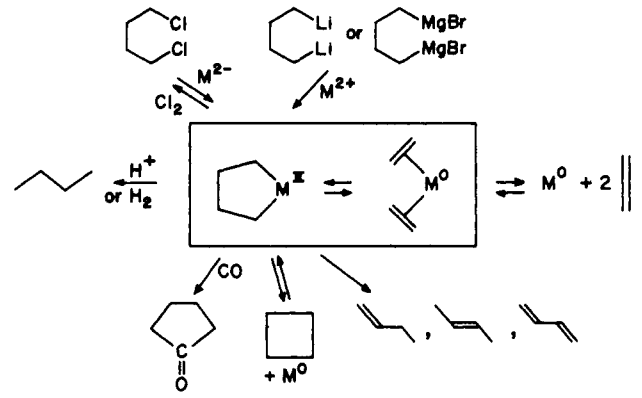

Scheme II

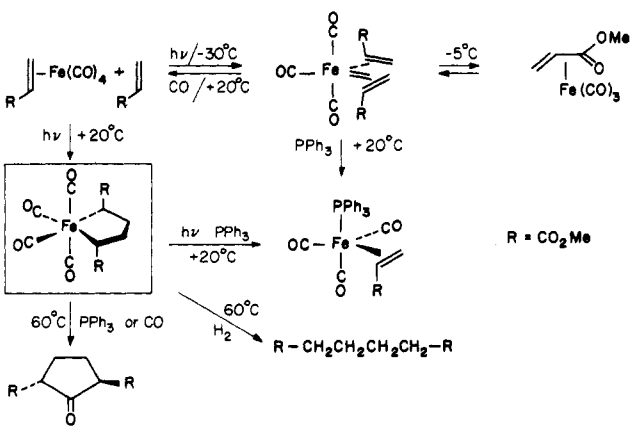

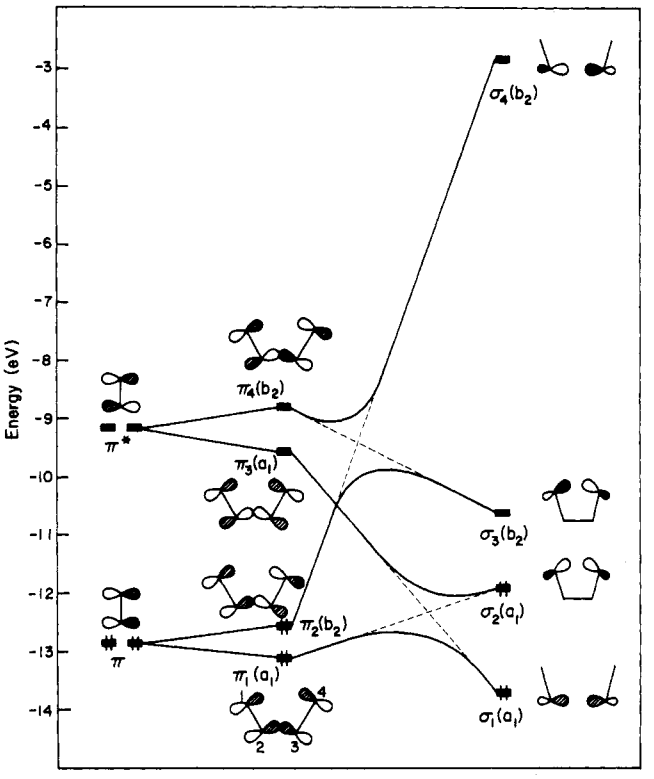

Figure 1. The orbitals of two ethylenes (left) interact to give the delocalized combinations in the middle. The correlation diagram is to a tetramethylene at right with a diradical a_1 level below b_2.

In this paper we begin a theoretical analysis of the stereochemistry of the metallacyclopentane–bisolefin interchange, focusing on the iron tricarbonyl system.[17]

The Uncatalyzed Reaction

Bringing up two ethylenes to each other in a $[_\pi 2_s + _\pi 2_s]$ geometry is a forbidden reaction.[18] Canting them away from each other as they approach, as in **4** → **5**, may or may not remove this stricture. Let us examine this process.

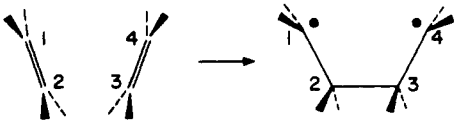

As the two ethylenes approach each other the pairwise degeneracy of their π and π^* levels breaks down, and four distinct levels, conveniently labeled π_1, π_2, π_3, and π_4 at the left of Figure 1, appear. The energy separation between π_1 and π_2 and between π_3 and π_4 increases rapidly. The orbitals transform continuously into those of a tetramethylene diradical, and in doing so localize appreciably but not entirely in the σ bond (C_2 and C_3) or the radical sites (C_1 and C_4). The localization could be viewed alternatively as a polarization phenomenon within one fragment—π and π^* mixing through their mutual interaction with orbitals of the other ethylene,[19] schematically shown in **6**—or as the symmetry-enforced mixing of delocalized orbitals, π_1 with π_3, π_2 with π_4, as drawn in **7**.

On the other side of the correlation diagram is tetramethylene.[20] The ordering of the symmetric and antisymmetric radical lobe combinations, σ_2 and σ_3, in this molecule depends strongly on the interior C_1–C_2–C_3 angle α. If this angle is large, σ_2 and σ_3 will change place in energy,[20] and the crossing indicated in Figure 1 will not take place. However, we are not working with a free diradical, but one constrained to chelate a metal atom. From the crystal structures available to us of metallacyclopentanes[3c,7,8b,11g,h,16] and bisolefin complexes[21]

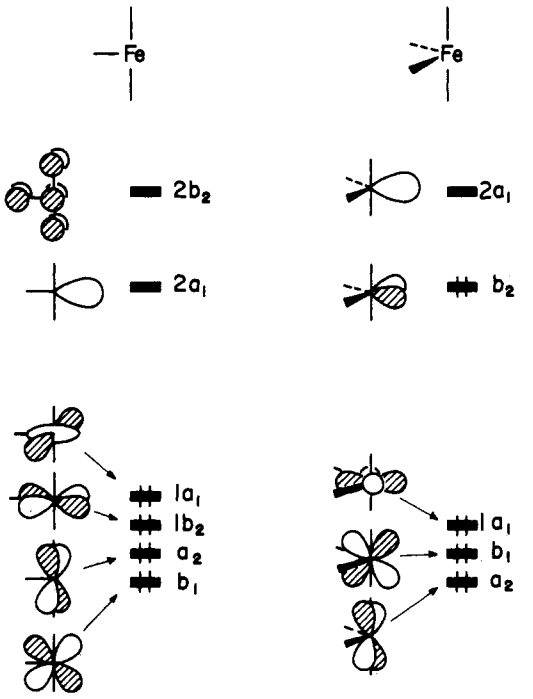

Figure 2. The orbitals of $Fe(CO)_3$ and $Fe(CO)_4$ fragments. The vertical energy scale is schematic.

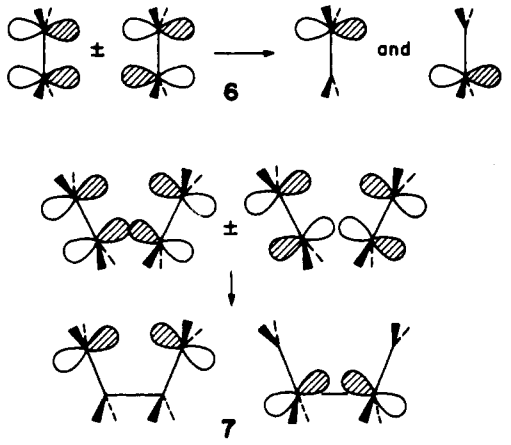

we judge that the tetramethylene fragment geometry in a complex is such that the symmetric radical combination σ_2 is at a lower energy. This is what is shown in Figure 1. The consequences are a level crossing along the bond forming reaction coordinate.

Therefore, if the metal + ligand complex retains the C_{2v} symmetry of the C_4H_8 ligand, and the metal merely acts as a template, the reaction remains forbidden in the classical sense. The transformation will require a sizable activation energy. The barrier height may be abolished or decreased either by substantial electron flow accompanied by level reordering in the process of metal complex formation or by a large distortion in symmetry in the course of the reaction. We will see that both factors enter the picture.

The Bisethylene Iron Tricarbonyl Ring Closure Reaction

Although the molecular structure of the title compound is unknown, there are sufficient experimental[14a] and theoretical[22] indications to assume that it has a C_{2v} trigonal bipyramidal conformation **8**, in which two ethylenes lie close to or in the equatorial plane. Only steric exigencies might affect this equilibrium orientational preference. Using **8** as the starting material—though it does not matter which end of the reaction one starts at—one is led to consider, on the basis of previous

Scheme III

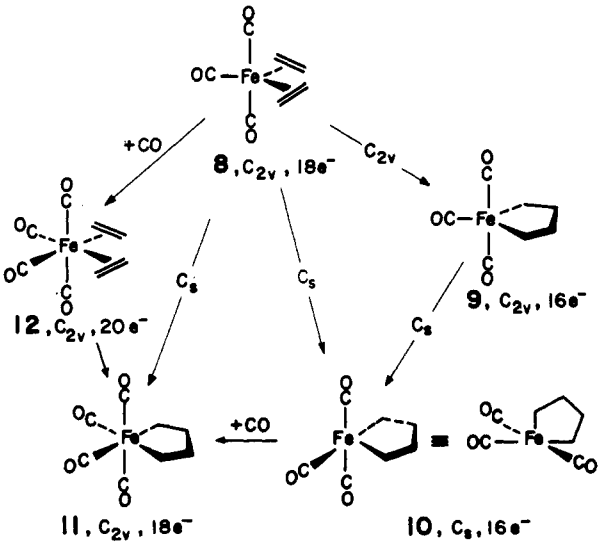

experience, several alternative pathways to the end point, the tetracarbonyl ferracyclopentane **11**. These are illustrated in Scheme III.

The basic questions are the relative timing of the CC bond formation and carbonyl addition and the geometry of the possible electron-deficient intermediates. Addition of CO prior to cyclization, **8** → **12**, leads to an unlikely 20-electron intermediate. A more realistic sequence would begin with a CC bond forming step retaining C_{2v} symmetry, to give the coordinatively unsaturated **9**. Whenever one has a d^6 five-coordinate molecule one had better worry about distortions away from a trigonal bipyramid,[22,23] for instance, to the square-pyramidal **10** or to an isomer thereof with the tetramethylene spanning basal positions of a square pyramid. If **10** is more stable than **9**, as will turn out to be the case, one must consider a direct pathway of low C_s symmetry for **8** to **10**. Addition of CO completes the reaction. Finally, one needs to consider the path **8** to **11**, in which all motions, CC bond formation, skeletal deformation, and CO addition are concurrent.

We have examined all these possibilities using the extended Hückel method, with parameters specified in the Appendix. The geometrical motions are complex. Three angular parameters were found to be convenient in defining a reaction coordinate. They are shown in a "top" view, along the axis of the trigonal bipyramid, in **13**. The CH_2 groups were oriented

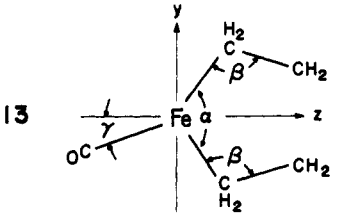

so as to follow the ring closure. Geometrical details are provided in the Appendix.

Let us begin with the electronic structure of the reactants and products, **8**–**11**. It is useful to have in hand the orbitals of $Fe(CO)_3$ and $Fe(CO)_4$ fragments. These are shown schematically in Figure 2, and have been described in detail elsewhere.[23a,24] There is a typical pattern of three low-lying orbitals in ML_4, four such in ML_3, these orbitals being primarily metal d. Above them lies a single well-directed hybrid $2a_1$ in $Fe(CO)_3$ and a pair of such hybrids $2a_1 + b_2$ in $Fe(CO)_4$. In $Fe(CO)_3$ there is another orbital, $2b_2$, at only slightly higher energy than $2a_1$. $2b_2$ is mainly a carbonyl orbital[25] and so mixes less with the organic ligand to be brought in. The electron count is such that the low-lying block is precisely filled in $Fe(CO)_4$,

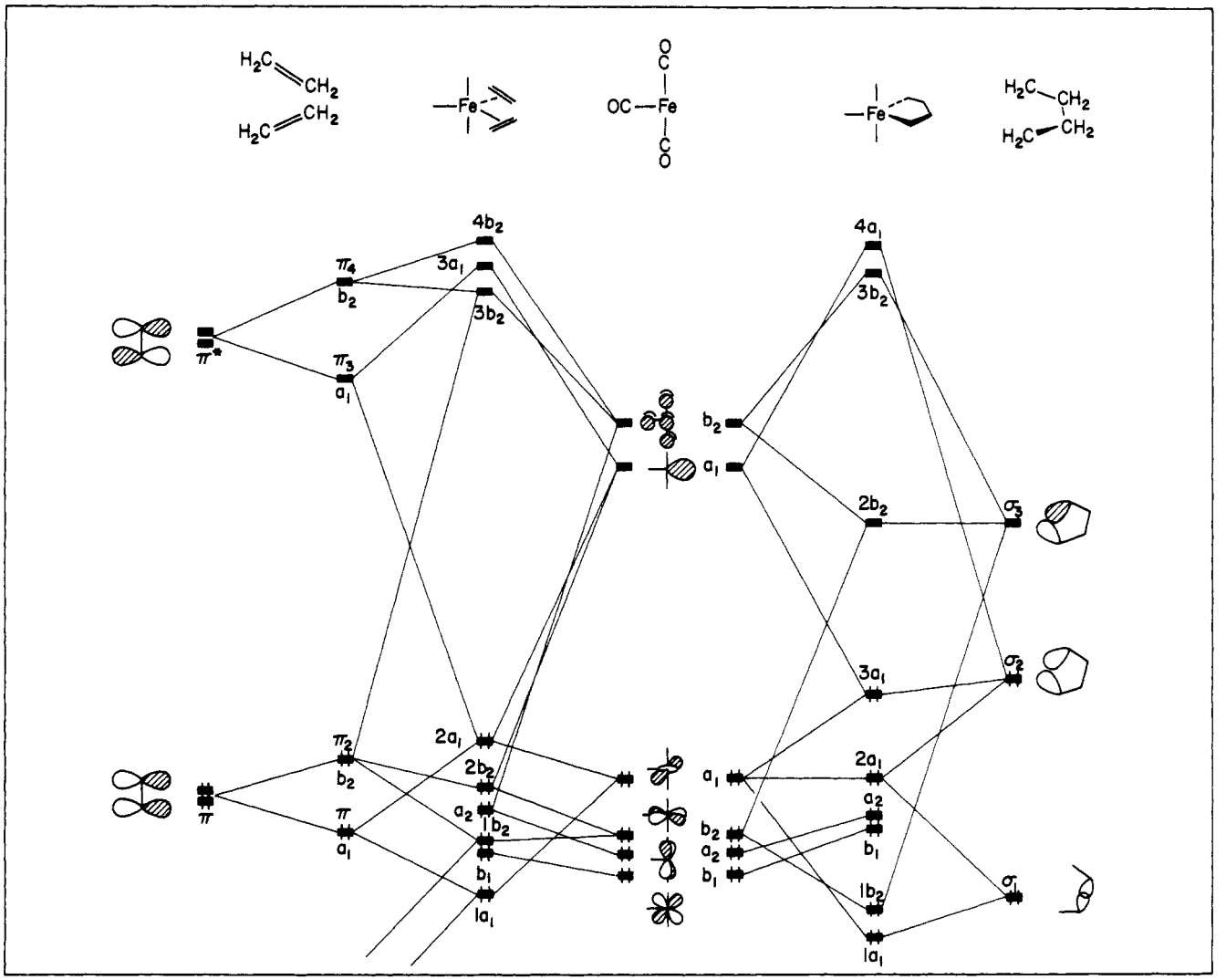

Figure 3. Construction of the orbitals of $(CO)_3Fe(ethylene)_2$, at left, and $(CO)_3Fe(tetramethylene)$, at right.

but in $Fe(CO)_3$ room must be found for two more electrons. A consequence of this is that $Fe(CO)_3$ complexes are much more dependent on the acceptor capability of the incoming ligand.

The construction of the orbitals of the bisethylene and tetramethylene complexes of $Fe(CO)_3$, **8** and **9** of Scheme III, is given in Figure 3. $Fe(CO)_3(ethylene)_2$ is a normal 18-electron complex. The donor orbitals of the two ethylenes interact effectively with $2a_1$ and $2b_2$ of $Fe(CO)_3$ and a large gap between filled and unfilled orbitals is produced. This is not the case for the tetramethylene complex. The gap between filled and unfilled orbitals is not large. It can (and will) be increased by a deformation of $a_1 \times b_2 = b_2$ symmetry, which corresponds to a motion which will take it to the square-pyramidal **10**.[26]

There is another view of these systems that it is interesting to pursue here. Both are trigonal-bipyramidal complexes. The expected level splitting pattern for ML_5 is the familiar e″ below e′ below a_1' shown below in **14**. Note the coordinate system has

14

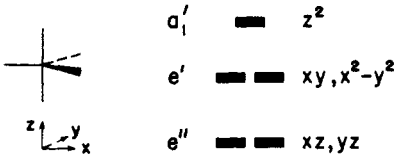

the z axis along the threefold axis. Both the bisolefin complex and the metallacyclopentane are not ML_5 but a strong perturbation thereon, ML_3L_2'. In the reduced C_{2v} symmetry it is natural to reorient the axes, as shown in **15**. The correlations are e″ → $b_1 + a_2$, e′ → $a_1 + b_2$.

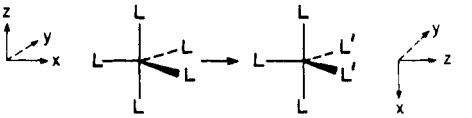

15

To what extent do the bisethylene and metallacycle electronic structures reflect their trigonal-bipyramid origins? The e″ → $b_1 + a_2$ levels are not strongly affected by π bonding, nor much by σ bonding differences in the equatorial planes, and they do not split much in energy. On the other hand, the perturbation is severe on the e′ → $a_1 + b_2$ set. In the bisethylene complex, they may be identified with $2a_1$ and $2b_2$ though delocalization is extensive. Both are stabilized by interaction with ethylene π^* levels to the extent that they approach in energy the b_1 and a_2 orbitals descended from e″. In the metallacycle the mixing is substantial again, and complicates the situation. Two localized metal to tetramethylene σ bonds would transform as $a_1 + b_2$. The new localized C_2–C_3 σ bond is a_1. Metal–ligand and CC σ bonds mix, in the a_1 species especially. To complicate matters the metal e′ d orbitals are also $a_1 + b_2$. With some oversimplification the mixing may be unraveled as follows: $1a_1$ and $2a_1$ of the metallacycle side of Figure 3 are mixtures of C_2–C_3 σ bonding and metal–C_1, C_4 bonding. $1b_2$ is also metal–C_1, C_4 bonding. The main metal contributions, the descendants of e′ in ML_5, are to be found in $3a_1$ and $2b_2$. These orbitals are shown in **16**. $3a_1$ is below $2b_2$, and one way

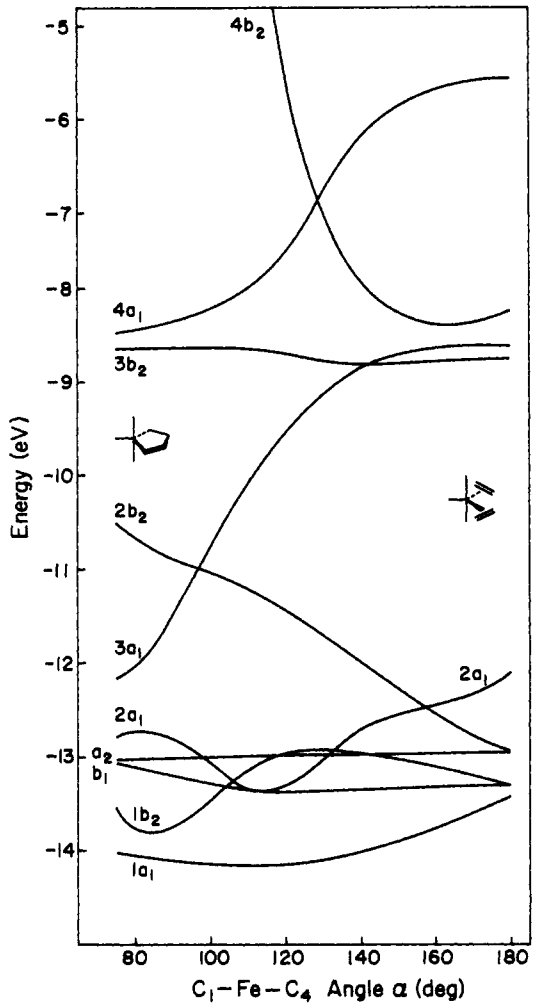

Figure 4. The evolution of the orbital energies along a C_{2v} pathway connecting **8** and **9**. The primary reaction coordinate α is defined in **13**—it is the C-Fe-C angle. The highest occupied level is $2a_1$ or $2b_2$ on the bisolefin side, $3a_1$ on the tetramethylene side.

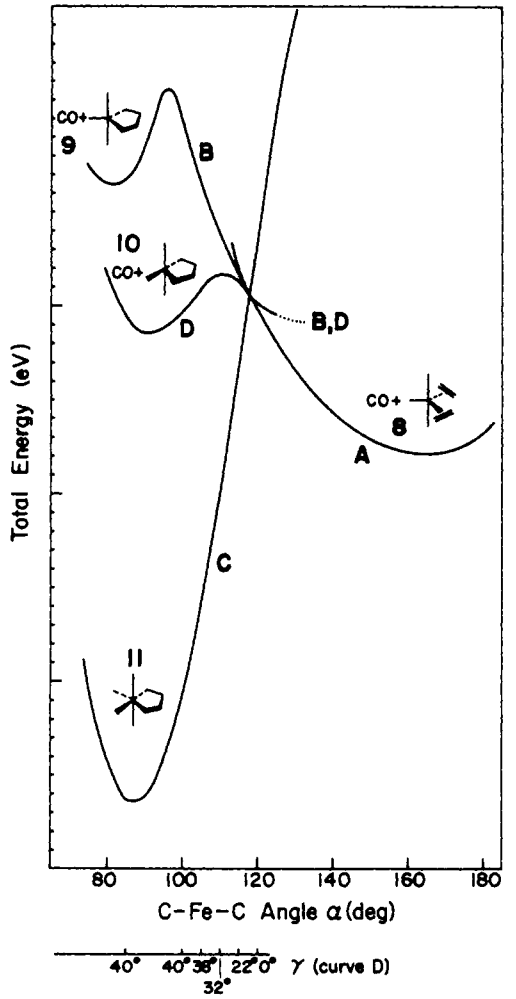

Figure 5. Several computed reaction paths. Curve A begins from the bisethylene **8**, curve B from the coordinatively unsaturated tetramethylene complex **9**, curve C from the product $Fe(CO)_4$ metallacycle **11**. In these curves C_{2v} symmetry is maintained. In curve D a less symmetrical C_s path from **10** is explored. The vertical energy scale markings are in eV.

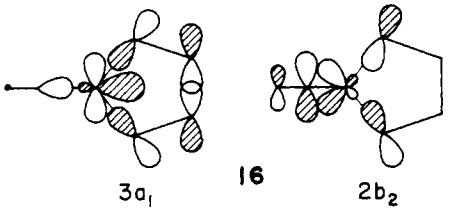

to rationalize this order is to argue that the tetramethylene radical lobes are better σ donors than the carbonyl lone pair. In the two e′ components the a_1 is primarily influenced by the σ donor capability of the unique ligand (CO), while the energy of b_2 is set by the σ donor strength of the other two equatorial ligands.

Is the simple C_{2v} metallacycle formation **8** $\rightleftarrows$ **9** an allowed

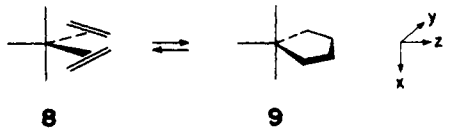

reaction? On the bisolefin side the two π bonds transform as $a_1 + b_2$, the four metal d orbitals as $a_1 + a_2 + b_1 + b_2$. On the metallacyclopentane side we have already said that the new CC bond and the metal-ligand σ bonds transform as $a_1 + b_1 + a_1$, in this d^6 16-electron complex. So the reaction will be a forbidden one, and in making it such the ordering of the levels descended from e′, $a_1(3a_1)$ below $b_2(2b_2)$ is crucial. Were the ordering reversed (and perhaps we should think about a strategy for achieving that situation) the reaction would be allowed.

The details of the level crossing and its consequences for the configuration energy may be seen in Figures 4 and 5. We have studied the reaction profile in some detail, varying the three crucial angles α, β, and γ of **13**. It was found that α dominated the reaction coordinate, at least in its initial stages, so that the plots are of a slice of the surface where α is varied at optimum β. Note that the level crossing occurs at $\alpha \sim 100°$, late in the reaction. This will be important in the sequel.

When relaxation of the equatorial CO angle γ is permitted, the trigonal-bipyramidal 16-electron ferracyclopentane **9** indeed is unstable toward deformation in the direction of a square-pyramidal isomer **10**. The single most important sta-

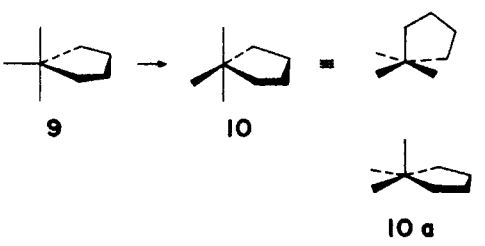

bilizing contribution in this process is the mixing of the frontier orbitals, $2b_2$ and $3a_1$ of Figure 4, now both a′ in the reduced

C_s symmetry. The LUMO of **10** becomes ideally hybridized to receive the lone pair of an incoming fourth carbonyl, as shown below.

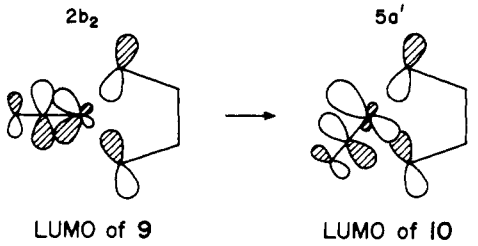

Not only is the square-pyramidal isomer **10** more stable, but the activation energy to reach it from the bisethylene is lowered, relative to **9**. This we learned from a study of the C_s reaction path connecting **10** and **8**, curve D of Figure 5.

Another square-pyramidal isomer, **10a**, tetramethylene spanning two basal sites, is much less stable than **10**. This is in accord with the predicted substituent preference pattern for five coordination;[22] i.e., better σ donors should prefer apical sites. **10a** appears to be a dead end, for there are high barriers blocking carbon–carbon bond cleavage in this isomer.

While the square-pyramidal $Fe(CO)_3$(tetramethylene) is stable, it is still coordinatively unsaturated. A great stabilization (~2.5 eV in our calculations) follows upon the addition of another carbonyl group to give the 18-electron, octahedral tetracarbonyl ferracyclopentane, **11**. Because the extended Hückel method is not reliable for bond-forming and -breaking steps, we have not studied the complete less symmetrical surface for carbonyl attack on the bisethylene $Fe(CO)_3$. Instead we have approached the transition-state region from all sides: in curve A in Figure 5 from the bisethylene–$Fe(CO)_3$, in curve B from the trigonal bipyramidal $Fe(CO)_3$ metallacycle, in curve D from the more stable square-pyramidal tricarbonyl, and in curve C from the product. As may be seen from Figure 5 all of these curves meet in the same region, a C_{2v} geometry with $\gamma = 0°$ near $\alpha = 118°$. The approach to the same energy and geometry from several diverse starting points gives us some confidence that we have located the approximate transition state for the reaction. We do not think that much will be changed in the full potential-energy surface—the acceptor orbital of the coordinatively unsaturated $Fe(CO)_3$ complexes is not so fully developed as to provide good interaction for an incoming CO until α is less than 110°, i.e., to the left of the transition state in Figure 5.

An important feature of the transition-state region is that it occurs still in the regime of approximate trigonal-bipyramidal coordination of iron. This will allow us to use a simple C_{2v} ring closure—paths A and B in Figure 5—to approximate a reaction path. The focus will not be on the trigonal-bipyramidal metallacyclopentane extreme of **9** but on the transition-state region near $\alpha = 120°$.

Along such a C_{2v} transit the heavy atom overlap populations evolve as shown in Figure 6. The C_1–C_2 bond weakens from a double bond to a single bond, one Fe–C_1 bond strengthens, the other Fe–C_2 weakens, and the largest incremental change occurs in the new C_2–C_3 bond. This is the basis of an analysis of stereoselectivity in cyclization of asymmetric olefins, which we treat next.

Unsymmetrical Olefins as Substrates

The coupling reaction of two asymmetric ethylenes can result in three distinct linkage isomers, **17a–c**. The known reactions are usually very selective if not stereospecific, and their selectivity cannot always be accounted for by steric effects. The nature of the stereoelectronic control is our next topic.

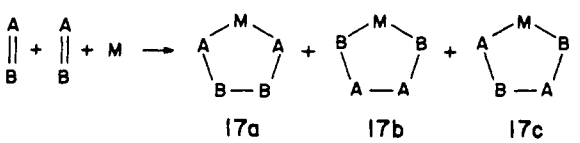

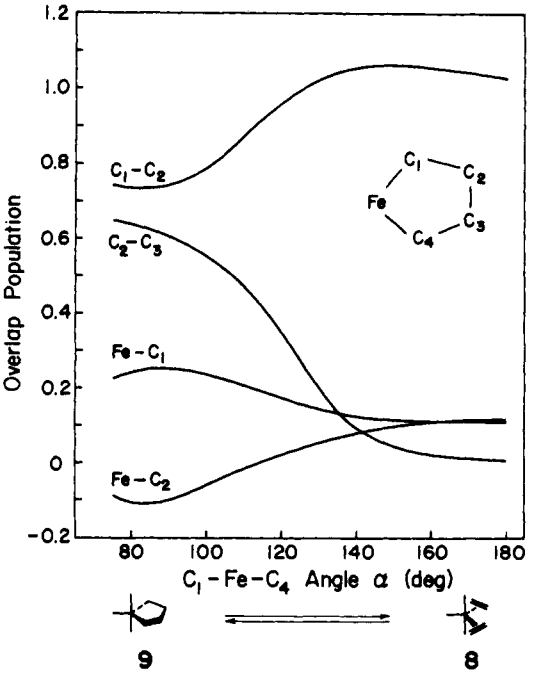

Figure 6. Overlap populations along a C_{2v} reaction path.

To obtain a model of olefin polarization without having to be concerned by concomitant steric effects we have modified the Coulomb integral of the 2p atomic orbital on each ethylene carbon by ±0.8 eV. The carbon with the higher H_{ii} of course becomes more positive, **18**, and the ethylene π and π^* levels are polarized in an understandable way,[19,27] as in **19**. The π orbital is concentrated on the more electronegative atom, the π^* on the less electronegative one. The polarized ethylene models both substitution of heteroatoms for carbon (an atom more electronegative than carbon substituted for C_2) or substituents on the carbon atoms (π donors at C_1, π acceptors at C_2)[19].

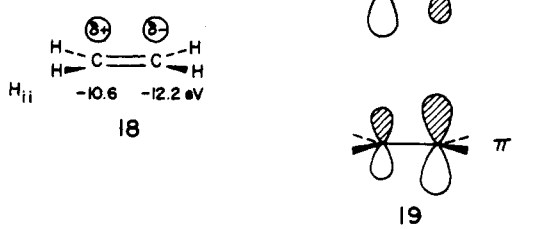

Separate potential energy surfaces, $E = f(\alpha, \beta, \gamma)$, were computed for the symmetric "isomers" **8a** and **8b**. The results are shown in Figure 7. A few points were also calculated for the asymmetrical **8c**, to ensure that its energy was intermediate between the symmetrical **a** and **b**. It was.

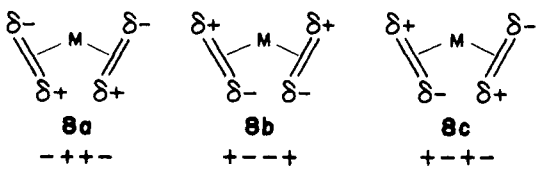

The computed cyclization barrier for isomer **8a** is significantly lower than for **8b**. As we shall soon see, this is in conformity with most experience.

Let us analyze the differences. On the metallacyclopentane side there is a trans effect at work. The −++− tetramethylene

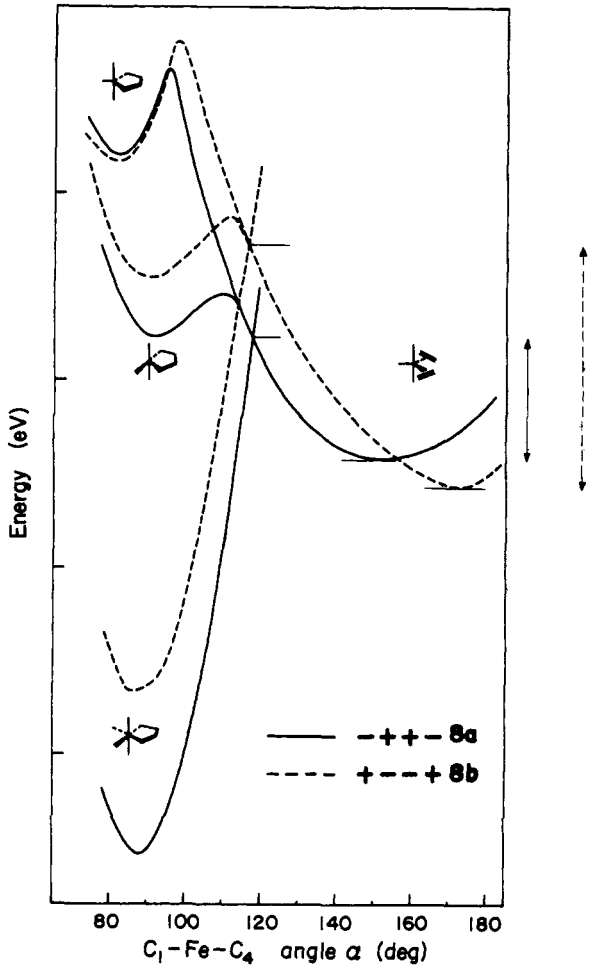

Figure 7. Some computed reaction paths for a model unsymmetrical ethylene. The solid line is for a −++− arrangement, **8a**, the dashed line for +−−+ **8b**.

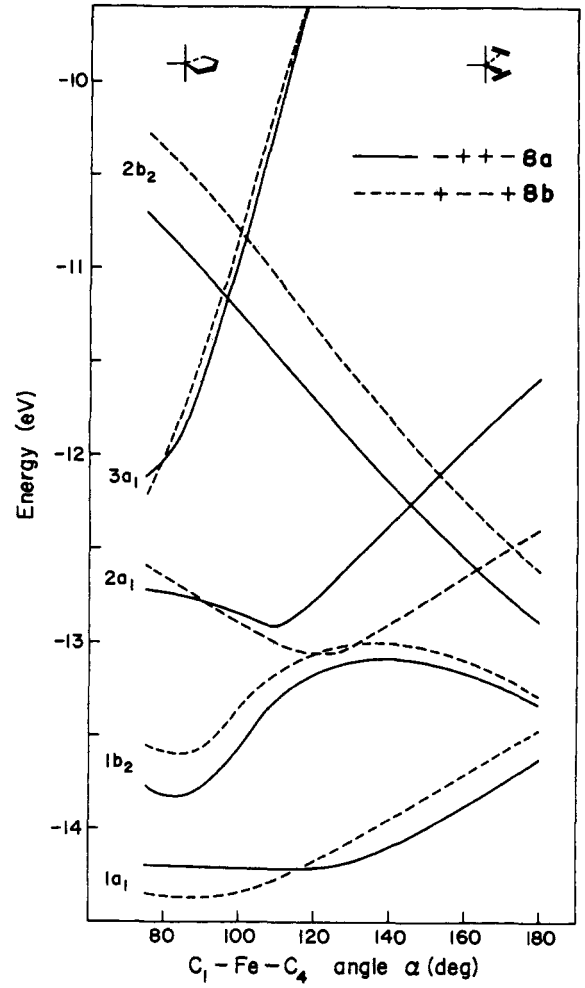

Figure 8. Energy for a_1 and b_2 frontier orbitals along a C_{2v} reaction path. The solid line is for a −++− arrangement, **8a**, the dashed line for +−−+ **8b**.

(the mnemonic notation refers to the electronegativity changes in the original ethylene, and is given in structures **8a–c**) is a poorer donor at its termini than +−−+. It therefore is stabilized to a greater extent by trans carbonyls, of which there are more in **11** than in **10**.

At equilibrium α is significantly smaller for **8a** (152°) vs. **8b** (172°). This is a consequence of the steric crowding, a four-electron repulsive interaction between π orbitals. The π_1 and π_2 combinations are shown in **20**. The polarization clearly

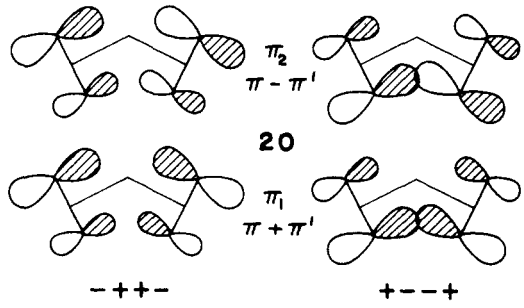

produces less interaction, therefore less destabilization, in the −++− case.

This effect is supplemented by another one. To the extent that bonding to the metal is effective there will be some population of π_3 as well. As shown in **21**, this is accentuated in the −++− isomer.

The prediction of a lower activation energy for the −++− cyclization is quite clear from Figure 7. While we understand the gross result from the preceding arguments, it would be

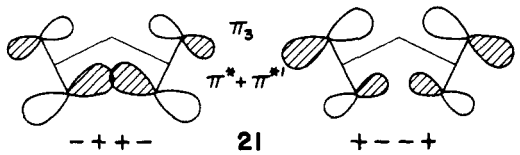

useful to determine whether π or π^* polarization dominated, or if both are equally important. Our modeling so far has perturbed both π and π^*, and in opposite directions. Yet we know that there are olefins in which the polarization is in the same direction for π and π^*, for instance, butadiene. Let us probe this point farther.

The evolution of the frontier orbitals of the system along an approximate reaction coordinate is illustrated in Figure 8. Note the following features: (1) Initially, on the bisethylene side, all the b_2 levels, C_2–C_3 antibonding, head up in energy; all the a_1 levels, C_2–C_3 bonding, are stabilized. (2) Initially again, all the a_1 levels are higher in energy for the −++− isomer, all the b_2 levels lower. That follows from the polarization in the π levels and the bonding or antibonding character of the levels. Both features point to the importance of establishing C_2–C_3 bonding early along the reaction coordinate. This in turn is obvious from Figure 6 presented earlier and is consistent with the known energetics of CC vs. C–metal bond formation[28] (Table I).

The controlling orbital, not surprisingly, is the HOMO on the bisethylene side, $2a_1$. It is strongly involved in C_2–C_3 bond formation. As **22** shows, $2a_1$ evolves from a 1:1 M:ligand combination to an orbital mainly on the ligands, strongly

Table I. Approximate Enthalpies of X-C Bond Formation (kJ/mol)[a]

C-C	~350	$Mn-CH_3$	117
Fe-CO	118	$M-C(O)C_6H_5$	105
$Fe-C_2H_4$	96		

[a] After ref 28.

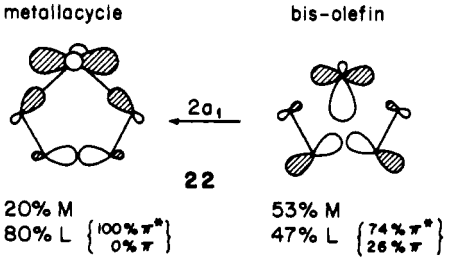

C_2–C_3 bonding. The composition of its ligand part is dominated by π^* and grows as the metallacycle is formed. Although less stable initially in the −++− isomer, it is much more rapidly stabilized, since the π^* orbital in this isomer has its largest lobes in the β position, at C_2 or C_3.

The differential between the cyclization modes is spread out over many molecular orbitals. Nevertheless we feel confident that the activation energy is dominated by C_2–C_3 bond formation. That in turn requires occupation of π^* levels through the intermediacy of the metal. The π^* mixing is enhanced when the large lobes of the polarized π^* face each other in the β positions. The stereoelectronic control is summarized in **23**.

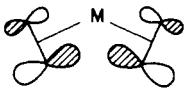

23

It confirms the previous qualitative analysis of Laszlo, Weissberger, and one of us.[12d,e]

It is interesting to point out here that a stereoselection rule with similar consequences for uncatalyzed thermal [2 + 2] cycloadditions of substituted olefins has been derived by Minot and Nguyen.[29a]

Our considerations refer to the very specific if popular case of metallacycle formation from a d^8 bisolefin. Can they be generalized to other cyclizations, on metal centers with diverse electron counts? For a very different reaction, the insertion of ethylene into a Pt-H bond, we found that the presence or absence of a large activation energy depended strongly on the coordination number and geometry of the metal center.[29] There are experimental hints of a similar strong dependence in the reverse reaction to the one studied here, nickelacyclopentane fragmentation of two olefins, in the results of Grubbs and co-workers.[9b,c] We are studying the latter reaction, and when our study is complete we will be in a better position to judge the generality of the conclusions. For now we proceed to an analysis of the experimental data assuming that the specificities elucidated for iron tricarbonyl carry over directly to other metal centers.

Comparison with Experimental Observations

The range of substituted olefins that has been studied is wide. To test the validity of the generalization which concludes the last section we need the orbitals of these ethylenic substrates. We will show them schematically, but in each case there is a molecular-orbital calculation to support the indicated polarization.

As indicated in the Introduction (Scheme I), methyl acrylate reacts photochemically with $Fe(CO)_5$ to give an unstable bisolefin complex which rapidly cyclizes and stereospecifically yields tetracarbonyl(1,4-*trans*-bis(carbomethoxy)tetramethylene)iron (**24**).[14a,16] Considering the symmetry of the olefin π^* orbital **25**, this finding is in agreement with our expectations.

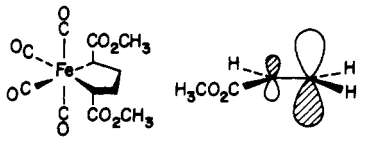

24 **25**

The cocondensation of methyl acrylate and butadiene on iron carbonyl presumably gives a solvated 16-electron ferracyclopentane **26**, which rearranges to give the π-allyl complex. The latter was analyzed by X-ray crystallography.[14b] Butadiene enters the metallacycle with the biggest lobe of its LUMO (**27**) β to the metal.

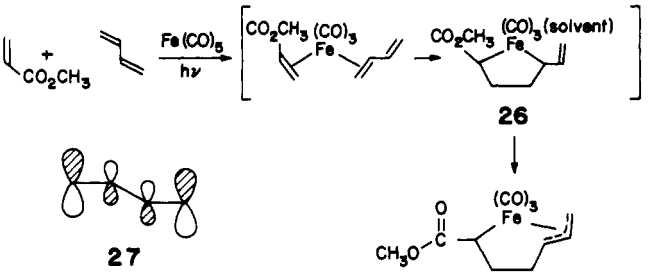

Butadiene itself reacts rapidly with bis(cyclooctadiene)-platinum to give a square-planar d^8 platinacyclopentane, **28**, which has trans α,α'-vinyl groups.[3c]

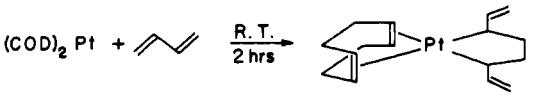

28

The tantalum carbene complex **29**, formally d^0, reacts with propene[6b] to form selectively a trans β,β'-dimethyltantalacyclopentane, **30**, in concordance with our predictions (see the polarization of the propene π^* orbital, **31**).

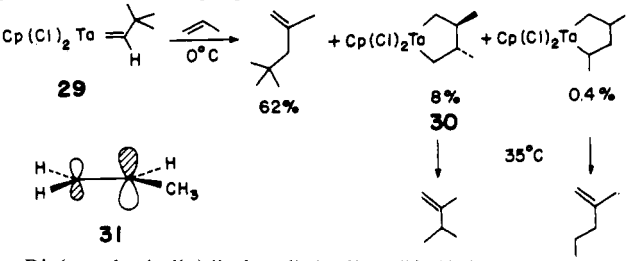

Bis(acrylonitrile)(indenyl)rhodium(I) (**32**), reacts with 2 mol of *tert*-butylacetylene to give **33**, the molecular structure of which was determined by X-ray crystallography.[30] The stereospecific formation of **33** can only result from a sequence of two specific couplings in which the π^* orbitals of the olefins have their largest lobes β to the metal (see **34** and **35**).

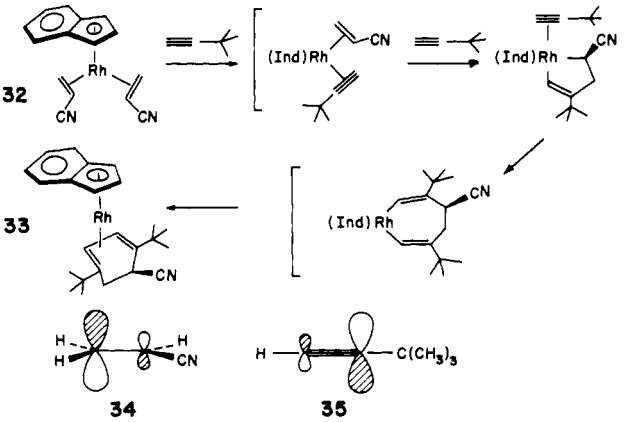

Norbornadiene and $Fe(CO)_5$ react with various polarized olefins[13] (methacrylonitrile, methacrylamide, and methyl acrylate) to give various coupling products which all have **36** as a common precursor.

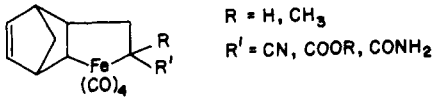

36

Norbornenone,[12c] 2-methylenenorbornene, and 2-ethylidenenorbornene[12f] react stereospecifically with $Fe(CO)_5$ to form syn-exo-trans-exo-syn ketones (**37**). Once more, the new CC bond is formed between the carbons carrying the biggest lobes of the olefinic π^* orbitals (**38**). The π and π^* orbitals of

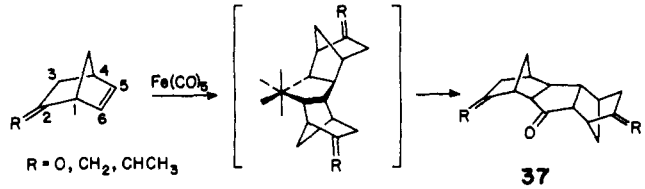

37

38

norbornenone are polarized in opposite directions, like those of methyl acrylate, while both π and π^* of alkylidenenorbornenes are polarized the same way, just as in butadiene. The stereospecificity observed in the case of methylenenorbornene is rather remarkable, given the very weak polarization of the double bond: C_5 and C_6 have ^{13}C chemical shifts of 134.4 and 136.6 ppm, respectively, compared to 143 and 130.8 ppm in norbornenone.

Green and his collaborators have studied extensively the coupling of fluorinated olefins on transition-metal complexes of iron(0)[31-33] and rhodium(I).[34] They proposed an ionic and a concerted mechanism as possible reaction pathways.[33] Several examples of stereospecific ferracyclopentane syntheses are shown below.[31-33] These concur with the π^* polarization

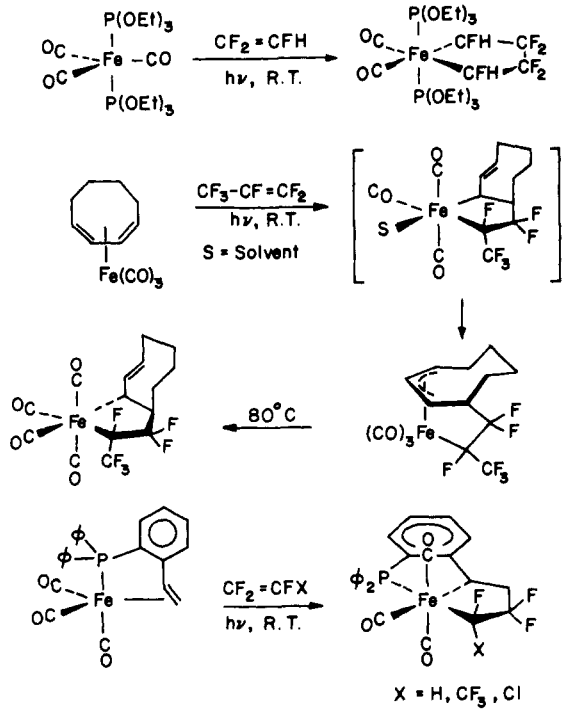

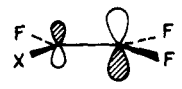

39

computed in **39**. Hexafluoroacetone, which can form π complexes, also behaves "normally" in its reaction with **40** (see **41**).[34]

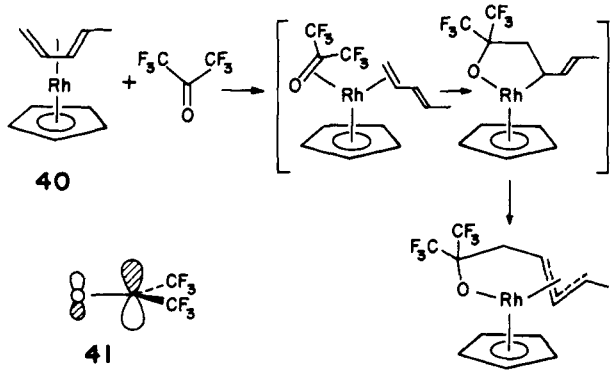

40

41

The transition metal catalyzed di- and trimerization reactions of acetylene have been extensively studied in recent years.[35] Trimethylsilyl- and bis(trimethylsilyl)acetylene are reagents of choice in this process because they do not form cyclobutadienes (which kill the catalyst) and because the silyl group can be easily removed.[35g] The polarization in alkyl- and silylacetylene π^* is calculated to be that shown in **42** and **43**.

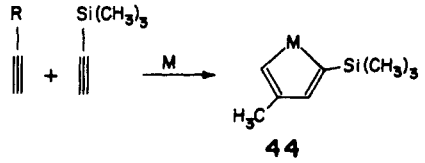

44

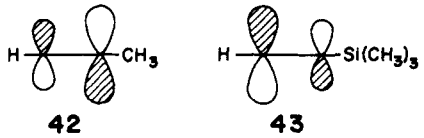

42 **43**

No experimental information is available on their condensation, to our knowledge. We would predict that the alkyl group would wind up in the β and the trimethylsilyl group in the α position, as in **44**.

Apparent Failures

The reaction of *trans*-cinnamaldehyde iron tri- and tetracarbonyl with C_2F_4[32] has no selectivity, producing a 4:5 mixture of **45** and **46**. Further, the trans olefin ends up in a cis

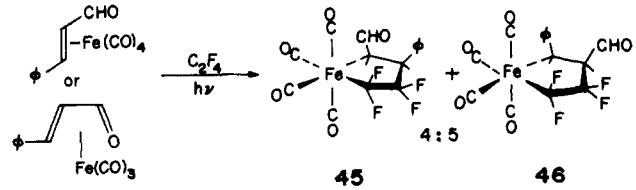

45 **46**

configuration. Considering the well-defined polarization of the π^* orbital in *trans*-cinnamaldehyde (**47**, all-planar conformation), this observation runs counter to our expectations for a kinetically controlled reaction product.

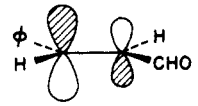

47

Grubbs and co-workers have found that bis(triphenylphosphine)nickelacyclopentane exchanges ethylene rapidly

with free olefins present in solution.[36] This means in other words that the cycloreversion or ring-opening reaction has a small activation energy in this case. Therefore one might expect the distribution of nickelacyclopentane isomers derived from $(PPh_3)_2Ni(CH_2)_4$ and propene to reflect more the thermodynamic equilibrium (dictated by methyl–methyl repulsions) than the kinetic selectivity in the ring-closure reaction. This is exactly what Grubbs observed (**48**, −20 °C, 63-fold excess

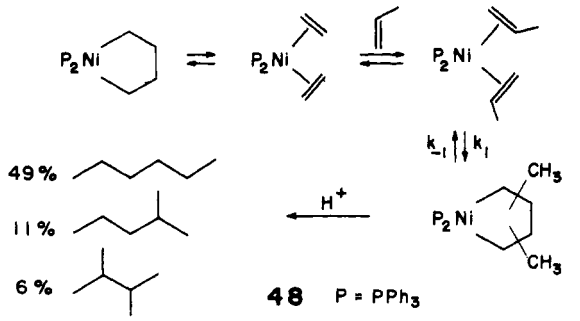

propene).[36] One would have observed exactly the opposite sequence if k_{-1} had been very small (cf. the tantalum case discussed above).

The reaction of hexafluoroacetone or its imine with **49**[37] may receive the same explanation, although the formation of **50**

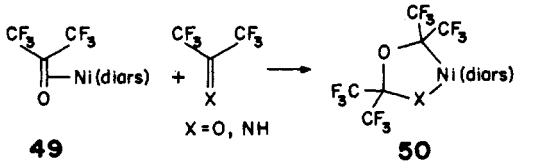

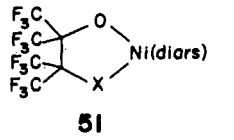

may also follow from an ionic addition. Normally we would have expected **51** as the main product (cf. **41**), but the steric repulsions between four eclipsed CF_3 groups would obviously be enormous. A head to head adduct of type **51** has indeed been observed recently in the reaction of platinum complexes with indan-1,2,3-trione.[38]

Steric constraints may also control the rapid reaction between methylenecyclopropane and $Ni(COD)_2$.[9a] In this reaction, **54** derives from metal insertion into the α cyclopropane

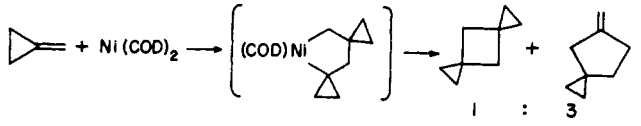

ring of **52**. From the direction of polarization in the cyclopropane π^* orbital, **55**, we would have expected **57** to be the main

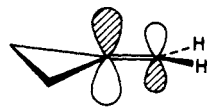

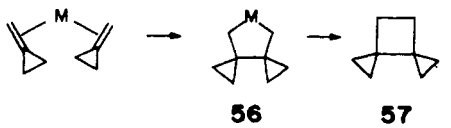

product of the reaction. Again we suspect that its formation is prevented by steric hindrance.

We think that the observed apparent exceptions to the π^* polarization rule are either the result of severe steric encumbrance or the consequence of reversible reactions with thermodynamic control products. The great majority of examples of this important reaction type follows a pattern which is in accord with our theoretical analysis.

Table II. Extended Hückel Method Parameters

orbital	H_{ii}, eV	exponent
H 1s	−13.6	1.3
C 2s	−21.4	1.625
2p	−11.4	1.625
N 2s	−26.0	1.95
2p	−13.4	1.95
O 2s	−32.3	2.275
2p	−14.8	2.275
F 2s	−40.0	2.425
2p	−18.1	2.425
Si 3s	−17.3	1.383
3p	−9.2	1.383
Fe 4s	−10.05	1.575
4p	−5.02	0.975
3d	−12.90	*a*

[a] For iron a linear combination of two 3d functions was used, one with exponent 5.35, coefficient 0.536 59, the other with exponent 1.8, coefficient 0.667 79.

Acknowledgment. We are grateful to the National Science Foundation for its support of this work through Research Grant CHE 7606099, and to the referees for correcting several errors. Our drawings are by J. Jorgensen, and the typing is by E. Stolz, both of whom we thank. The permanent affiliation of A.S. is with the Laboratoire de Chimie Organique Physique of the Université de Liege, Belgium.

Appendix

In the absence of a full potential energy surface search a number of geometrical assumptions had to be made. In the basic structures **8–11** the Fe-C_1-C_4 distances were held constant at 2.05 Å, while C_1-C_2 and C_3-C_4 were set at 1.40 Å in **8** and 1.54 Å in the ring-closed **9–11**.

In **8** the CH_2 bond angles were fixed at 115°, the H_2C_1 and H_2C_2 planes bisecting the Fe-C_1-C_2 and Fe-C_2-C_1 angles, respectively. In **9–11**, the CH_2 angles were 109.5°, the H_2C_1 plane bisected the Fe-C_1-C_2 angle, and the H_2C_2 plane bisected the C_1-C_2-C_3 angle. This rudimentary procedure allowed the hydrogen atoms to follow closely and automatically the ring closure and opening motions.

For each molecule, a minimum $E = f(\beta)$ was computed for a range of α values; β varied by 2° increments. The angle between the equatorial CO ligand and the x axis, γ, was set to zero for **8** and **9** and to 45° for **11**. A special procedure was used for **10**: an $E = f(\alpha,\beta)$ curve was computed with γ held constant at 45°; then γ was optimized for each (α, best β) set derived from the previous calculation.

Our calculations were of the extended Hückel type,[39] with a weighted H_{ij} formula.[40] The parameters, standard ones for first-row atoms, are listed in Table II. To model a polarized olefin the carbon 2p H_{ii}'s were modified as indicated in the main body of the text.

References and Notes

(1) (a) Manuel, T. A.; Stafford, S. L.; Stone, F. G. A. *J. Am. Chem. Soc.* **1961**, *83*, 249–250. (b) Coyle, T. D.; King, R. B.; Pitcher, E.; Stafford, S. L., Treichel, P.; Stone, F. G. A. *J. Inorg. Nucl. Chem.* **1961**, *20*, 172–173.
(2) Hoehn, H. H.; Pratt, L., Watterson, K. F.; Wilkinson, G. *J. Chem. Soc.* **1961**, 2738–2745.
(3) (a) Cundy, C. S.; Green, M.; Stone, F. G. A. *J. Chem. Soc. A* **1970**, 1647–1653. (b) Ashley-Smith, J.; Green, M.; Stone, F. G. A. *Ibid.* **1969**, 3019–3023. (c) Barker, G. K.; Green, M.; Howard, J. A. K.; Spencer, J., Stone, F. G. A. *J. Am. Chem. Soc.* **1976**, *98*, 3373–3374.
(4) (a) Cassar, L.; Eaton, P. E.; Halpern, J. *J. Am. Chem. Soc.* **1970**, *92*,

3515–3518. (b) Eaton, P. E.; Patterson, D. R. *Ibid.* **1978,** *100,* 2573–2575. (c) Sohn, M.; Blum, J.; Halpern, J. *Ibid.* **1979,** *101,* 2694–2698, and references cited therein.
(5) (a) McDermott, J. X.; Whitesides, G. M. *J. Am. Chem. Soc.* **1974,** *96,* 947–948. (b) McDermott, J. X.; White, J. F.; Whitesides, G. M. *Ibid.* **1976,** *98,* 6521–6528. (c) McDermott, J. X.; Wilson, M. E.; Whitesides, G. M. *Ibid.* **1976,** *98,* 6529–6536.
(6) (a) McLain, S. J.; Wood, C. D.; Schrock, R. R. *J. Am. Chem. Soc.* **1977,** *99,* 3519–3520. (b) McLain, S. J.; Schrock, R. R. *Ibid.* **1978,** *100,* 1315–1317.
(7) (a) Fraser, A. R.; Bird, P. H.; Bezman, S. A.; Shapley, J. R.; White, R.; Osborn, J. A. *J. Am. Chem. Soc.* **1973,** *95,* 597–598. (b) Diversi, P.; Ingrosso, G.; Lucherini, A.; Porzio, W.; Zocchi, M. *J. Chem. Soc., Chem. Commun.* **1977,** 811–812.
(8) (a) Harvie, I. J.; McQuillen, F. J. *J. Chem. Soc., Chem. Commun.* **1974,** 806–807. (b) Cheetham, A. K.; Puddephatt, R. J.; Zalkin, A.; Templeton, D. H.; Templeton, L. K. *Inorg. Chem.* **1976,** *15,* 2997–2999.
(9) (a) Binger, P. *Angew. Chem.* **1972,** *84,* 352–353. (b) Grubbs, R. H.; Miyashita, A.; Liu, M.-I.; Burk, P. L. *J. Am. Chem. Soc.* **1977,** *99,* 3863–3864; **1978,** *100,* 2418–2425. (c) Grubbs, R. H.; Miyashita, A. *Ibid.* **1978,** *100,* 1300–1302.
(10) (a) Evers, J. Th. M.; Mackor, A. *Tetrahedron Lett.* **1978,** 821–824.
(11) For some further examples see: (a) Cundy, C. S.; Lappert, M. F. *J. Organomet. Chem.* **1978,** *144,* 317–320. *J. Chem. Soc., Dalton Trans.* **1978,** 665–673, and references cited therein. Cundy, C. S.; Lappert, M. F.; Dubac, J.; Mazerolles, P. *Ibid.* **1976,** 910–914. (b) Vancea, L.; Graham, W. A. G. *Inorg. Chem.* **1974,** *13,* 511–513. (c) Eaborn, C.; Metham, T. N.; Pidcock, A. *J. Chem. Soc., Dalton Trans.* **1975,** 2212–2214. (d) Fink, W. *Helv. Chim. Acta* **1975,** *58,* 1464–1465. (e) Diversi, P.; Ingrosso, G.; Lucherini, A. *J. Chem. Soc., Chem. Commun.* **1977,** 52–53; **1978,** 735–736. (f) McAlister, D. R.; Erwin, D. K.; Bercaw, J. E. *J. Am. Chem. Soc.* **1978,** *100,* 5966–5968. (g) Bennett, M. A.; Johnson, R. N.; Tomkins, I. B. *Ibid.* **1974,** *96,* 61–69. (h) Hoffmann, K.; Weiss, E. *J. Organomet. Chem.* **1977,** *128,* 399–407.
(12) (a) Mantzaris, J.; Weissberger, E. *J. Am. Chem. Soc.* **1974,** *96,* 1873–1879, 1880–1884. *Tetrahedron Lett.* **1972,** 2815–2818. (b) Speert, A.; Gelan, J.; Anteunis, M.; Marchand, A. P.; Laszlo, P. *Ibid.* **1973,** 2271–2274. (c) Grandjean, J.; Laszlo, P.; Stockis, A. *J. Am. Chem. Soc.* **1974,** *96,* 1622–1623. (d) Stockis, A.; Weissberger, E. *Ibid.* **1975,** *97,* 4288–4292. (e) Weissberger, E.; Laszlo, P. *Acc. Chem. Res.* **1976,** *9,* 209–217, and references cited therein. (f) Weissberger, E.; Page, G. *J. Am. Chem. Soc.* **1977,** *99,* 147–151. (g) Stockis, A. Dissertation, Liège, 1977.
(13) Schmid, H.; Naab, P.; Hayakawa, K. *Helv. Chim. Acta* **1978,** *61,* 1427–1442.
(14) (a) Grevels, F.-W.; Schulz, D.; Koerner v. Gustorf, E. *Angew. Chem.* **1974,** *86,* 558–559. (b) Grevels, F.-W.; Feldhoff, U.; Leitich, J.; Krüger, C. *J. Organomet. Chem.* **1976,** *118,* 79–92.
(15) See also: (a) Steiner, U.; Hansen, H.-J. *Helv. Chim. Acta* **1977,** *60,* 191–203. (b) Lombardo, L.; Wege, D.; Wilkinson, S. P. *Aust. J. Chem.* **1974,** *27,* 143–152. (c) Bird, C. W. *Chem. Rev.* **1962,** *62,* 283–302. (d) Lemal, D. M.; Shim, K. S. *Tetrahedron Lett.* **1961,** 368–372. (e) Marchand, A.; Hayes, B. R. *Ibid.* **1977,** 1027–1030.
(16) Krüger, C.; Tsay, Y.-H. *Cryst. Struct. Commun.* **1976,** *5,* 215–218.
(17) For other theoretical studies of metallacyclopentane formation see: (a) Pearson, R. G. *Fortschr. Chem. Forsch.* **1973,** *41,* 75–112. Pearson, R. G. "Symmetry Rules for Chemical Reactions"; Wiley: New York, 1976; Chapter 5. (b) Braterman, P. S. *J. Chem. Soc., Chem. Commun.* **1979,** 70–71.
(18) Hoffmann, R.; Woodward, R. B. *J. Am. Chem. Soc.* **1965,** *87,* 2046–2048. Woodward, R. B.; Hoffmann, R. *Angew. Chem.* **1969,** *81,* 797–869.
(19) For a description of the polarization phenomenon see: Libit, L.; Hoffmann, R. *J. Am. Chem. Soc.* **1974,** *96,* 1370–1383, and references cited therein.
(20) (a) Hoffmann, R.; Swaminathan, S.; Odell, B. G.; Gleiter, R. *Ibid.* **1970,** *92,* 7091–7097. (b) Segal, G. A. *Ibid.* **1974,** *96,* 7892–7898.
(21) (a) Krüger, C.; Tsay, Y.-H. *J. Organomet. Chem.* **1972,** *34,* 387–395. (b) Jonas, K.; Pörschke, K. R.; Krüger, C.; Tsay, Y.-H. *Angew. Chem.* **1976,** *88,* 682–683.
(22) (a) Rösch, N.; Hoffmann, R. *Inorg. Chem.* **1974,** *13,* 2656–2666. (b) Rossi, A.; Hoffmann, R. *Ibid.* **1975,** *14,* 365–374, and references cited therein.
(23) (a) Elian, M.; Hoffmann, R. *Inorg. Chem.* **1975,** *14,* 1058–1076. (b) Burdett, J. K. *J. Chem. Soc., Faraday Trans. 2* **1974,** *70,* 1599–1613. *Inorg. Chem.* **1975,** *14,* 375–382. (c) Hay, P. J. *J. Am. Chem. Soc.* **1978,** *100,* 2411–2417. (d) Demuynck, J.; Strich, A.; Veillard, A. *Nouveau J. Chim.* **1977,** *1,* 217–228. (e) Lichtenberger, D. L.; Brown, T. L. *J. Am. Chem. Soc.* **1978,** *100,* 366–373.
(24) Albright, T. A.; Hoffmann, R.; Tse, Y.-C.; D'Ottavio, T. *J. Am. Chem. Soc.* **1979,** *101,* 3812–3821.
(25) It is composed of carbonyl π^*'s mixed in-phase with Fe 4p.
(26) This is an application of second-order Jahn–Teller arguments, for which see ref 17a.
(27) Heilbronner, E.; Bock, H. "Das HMO-Modell und Seine Anwendung"; Verlag Chemie: Weinheim/Bergstr., Federal Republic of Germany.
(28) Connor, J. A. *J. Organomet. Chem.* **1975,** *94,* 195–199.
(29) (a) Minot, C.; Nguyen, T. A. *Tetrahedron* **1977,** *33,* 533–537. (b) Thorn, D. L.; Hoffmann, R. *J. Am. Chem. Soc.* **1978,** *100,* 2079–2090.
(30) Caddy, P.; Green, M.; O'Brien, E.; Smart, L. E.; Woodward, P. *Angew. Chem.* **1977,** *89,* 671–672.
(31) Burt, R.; Cooke, M.; Green, M. *J. Chem. Soc. A* **1970,** 2975–2981.
(32) Bond, A.; Lewis, B.; Green, M. *J. Chem. Soc., Dalton Trans.* **1975,** 1109–1118.
(33) Green, M.; Lewis, B.; Daly, J. J.; Sanz, F. *J. Chem. Soc., Dalton Trans.* **1975,** 1118–1127.
(34) Green, M.; Lewis, B. *J. Chem. Soc., Dalton Trans.* **1975,** 1137–1142.
(35) (a) Collman, J. P.; Kang, J. W. *J. Am. Chem. Soc.* **1967,** *89,* 844–851. (b) Baddley, W. H.; Tupper, G. B. *J. Organomet. Chem.* **1974,** *67,* C16–C18. (c) Kolshorn, H.; Meier, H.; Müller, E. *Tetrahedron Lett.* **1971,** 1469–1472. (d) Chin, H. B.; Bau, R. *J. Am. Chem. Soc.* **1973,** *95,* 5069–5071. (e) Vollhardt, K. P. C.; Bergman, R. G. *Ibid.* **1974,** *96,* 4996–4998. (f) McAlister, D. R.; Bercaw, J. E.; Bergman, R. G. *Ibid.* **1977,** *99,* 1666–1668. (g) Funk, R. L.; Vollhardt, K. P. C. *Ibid.* **1977,** *99,* 5483–5484.
(36) Grubbs, R. H.; Miyashita, A. *J. Chem. Soc., Chem. Commun.* **1977,** 864–865.
(37) Browning, J.; Green, M.; Stone, F. G. A. *J. Chem. Soc. A* **1971,** 453–457.
(38) Hunt, M. M.; Kemmitt, R. D. W.; Russell, D. R.; Tucker, P. A. *J. Chem. Soc., Dalton Trans.* **1979,** 287–294.
(39) Hoffmann, R. *J. Chem. Phys.* **1963,** *39,* 1397–1412. Hoffmann, R.; Lipscomb, W. N. *Ibid.* **1962,** *36,* 2179–2189, 3489–3493; **1962,** *37,* 2872–2883.
(40) Ammeter, J. H.; Bürgi, H.-B.; Thibeault, J. C.; Hoffmann, R. *J. Am. Chem. Soc.* **1978,** *100,* 3686–3692.